

Electronic Supplementary Information

Change of Chemiresistive Properties Regulated by Nanoscale Curvature in Molecularly-Linked Nanoparticle Composite Assembly

Han-Wen Cheng^{a,b}, Shan Yan^b, Li Han^b, Yong Chen^a, Ning Kang^b, Zakiya Skeete^b, Jin Luo^b, and Chuan-Jian Zhong^{b*}

^a School of Chemical and Environmental Engineering, Shanghai Institute of Technology, Shanghai 201418, China

^b Department of Chemistry, State University of New York at Binghamton, Binghamton, NY13902, USA

Additional Descriptions of Theoretical Considerations and Experimental Data:

Estimation of the density of the nanocomposite: The density of multi-walled carbon nanotubes (MWCNTs, diameter ~26 nm) (NanoLab) is about 1.3 g/cm³.⁵² Consider a length of 10 nm CNT, the volume is 5309 nm³, the mass is 6.90 × 10⁻¹⁸ g, and the total surface area of one CNT is 817 nm². Consider gold nanoparticles of 2 nm core size capped with a full monolayer of decanethiolate (DT, molecular weight is 174.4 g/mol, length ~ 1.5 nm, diameter ~ 0.309 nm), the approximate projection area for one DT-Au_{nm} would be 25 nm². There would be ~132 DTs on one Au particle and ~33 (DT-Au_{nm}) on each CNT. Consider the density of gold (19.3 g/cm³), the total mass of DT-Au_{nm} + CNT, and the the total volume, the average density of (DT-Au_{nm})/CNT would be ~1.5 g/cm³.

Table S1. Average interparticle distances derived from analyses of the TEM data (Fig. 3).

Assembly	diameter (nm)	Interparticle Distance (<i>d</i>)	
		center-to-center <i>d_{cc}</i> (nm)	edge-to-edge <i>d_{ee}</i> (nm)
DT-Au _{nm}	1.8 ± 0.2	3.6 (± 0.4)	1.8 (± 0.3)
NDT-Au _{nm}	2.1 ± 0.4	3.6 (± 0.9)	1.5 (± 0.5)
NDT-Au _{nm} /CNTs	2.1 ± 0.3	5.0 (± 1.0)	2.9 (± 0.7)

Theoretical consideration of the electrical properties: The ratio of resistances before and after the change in radius of curvature can be expressed by the following equation (equation 1),⁴⁴

$$\frac{R_t}{R_i} = \exp[-\beta(d_1 - d_2)] \exp\left[\frac{0.5e^2}{4\pi\epsilon\epsilon_0RT} \left(\frac{1}{r+d_1} - \frac{1}{r+d_2}\right)\right] \quad (1a)$$

or in terms of relative resistance change,

$$\frac{R_t - R_i}{R_i} = \frac{\Delta R}{R_i} = \exp[-\beta(d_1 - d_2)] \exp\left[\frac{0.5e^2}{4\pi\epsilon\epsilon_0RT} \left(\frac{1}{r+d_1} - \frac{1}{r+d_2}\right)\right] - 1 \quad (1b)$$

where the resistance changes from R_i to R_t with interparticle distances change from d_1 to d_2 . β is the electron coupling term, r is the particle core radius, ϵ is dielectric constant of interparticle medium, and other parameters include $e = 1.6 \times 10^{-19}$ C, $\epsilon_0 = 8.854 \times 10^{-12}$ F/m, $R = 1.38 \times 10^{-23}$ J/K, and $T = 300$ K. The R_t to R_i ratio contains two exponential components. The first component is mainly determined by the interparticle distance change and the β value (“ β - d term”), whereas the second component is largely dependent on the particle size, interparticle distance change, and ϵ value (“ ϵ - r term”).

Considering $\Delta L/L = (d_2 - d_1)/(2r + d_1) = T_s/2R_b$, where L represents the length of the device whereas ΔL represents the change of the length upon strain. The corresponding interparticle edge-to-edge distances are d_1 and d_2 . For nanoparticle radius $r = 1$ nm, interparticle edge-to-edge spacing $d_1 = 1.6$ nm and $\beta = 4.0$ nm⁻¹,⁴⁴ the above two terms can be derived as a function of R_b based on a PET substrate of thickness $T_s = 125$ μ m⁴⁴ and a CNT wall thickness $T_s = 2$ nm (CNT: O.D. \times wall thickness $\times L$: (20-30 nm) \times (1-2 nm) \times (0.5-2 μ m)). Consider now the case of tensile strain, the radius of curvature for CNT would be 13 nm. Substituting these values into logarithm of equation-1, the two components can be expressed as a function of R_b (μ m in the equations):

$$"\beta - d" \text{ term} : -\beta(d_1 - d_2) = \frac{900}{R_b} \text{ (for } T_s = 125 \mu\text{m)}, \text{ or } \frac{0.0144}{R_b} \text{ (for } T_s = 2 \text{ nm)} \quad (2a)$$

$$"\varepsilon - r" \text{ term} : \frac{0.5e^2}{4\pi\varepsilon\varepsilon_0RT} \left(\frac{1}{r + d_1} - \frac{1}{r + d_2} \right) = \frac{27.8 \text{ nm}}{\varepsilon} \times \left(\frac{1}{2.6} - \frac{1}{2.6 + \frac{225}{R_b}} \right) \quad (2b)$$

Calculation of interparticle interaction potentials based on a dimer model: For a symmetric dimer, the steric repulsive and van der Waals attractive interaction energies as a function of interparticle edge-to-edge distance (d_{ee}) are given below:^{53,54}

$$E_{steric, sym} \approx \frac{100R_1\delta_{bruth}^3}{d_{ee}\pi\sigma_{thiol}^3} kT \exp\left(\frac{-\pi d_{ee}}{\delta_{bruth}}\right) \quad (3)$$

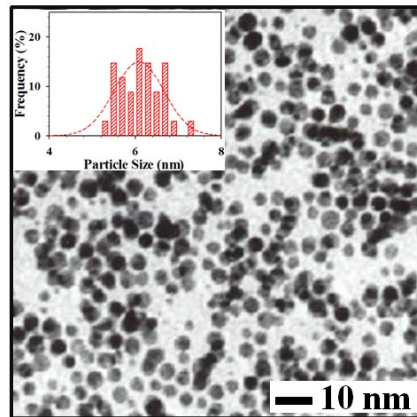
$$E_{vdW, sym} = \frac{A}{12} \left[\frac{4R_1^2}{(d_{ee} + 2R_1)^2 - 4R_1^2} + \frac{4R_1^2}{(d_{ee} + 2R_1)^2} + 2 \ln\left(\frac{(d_{ee} + 2R_1)^2 - 4R_1^2}{(d_{ee} + 2R_1)^2}\right) \right] \quad (4)$$

where R_1 is particle radius; δ and σ stand for the length and the diameter of a capping molecule on the nanoparticle surface. A is Hamaker constant.

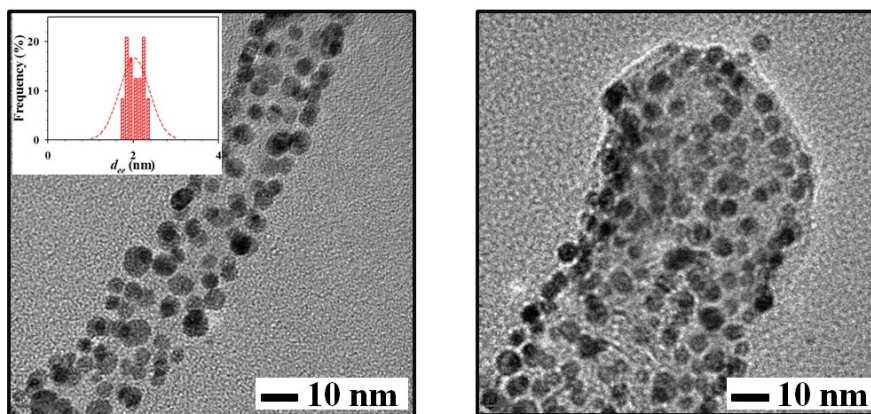
For an asymmetric dimer, the van der Waals attractive interaction energy as a function of interparticle edge-to-edge distance (d_{ee}) is given below:^{53,54}

$$E_{vdW, asym} = \frac{A}{6} \left[\frac{2R_1R_2}{(d_{ee} + R_1 + R_2)^2 - (R_1 + R_2)^2} + \frac{2R_1R_2}{(d_{ee} + R_1 + R_2)^2 - (R_1 - R_2)^2} + \ln\left(\frac{(d_{ee} + R_1 + R_2)^2 - (R_1 + R_2)^2}{(d_{ee} + R_1 + R_2)^2 - (R_1 - R_2)^2}\right) \right] \quad (5)$$

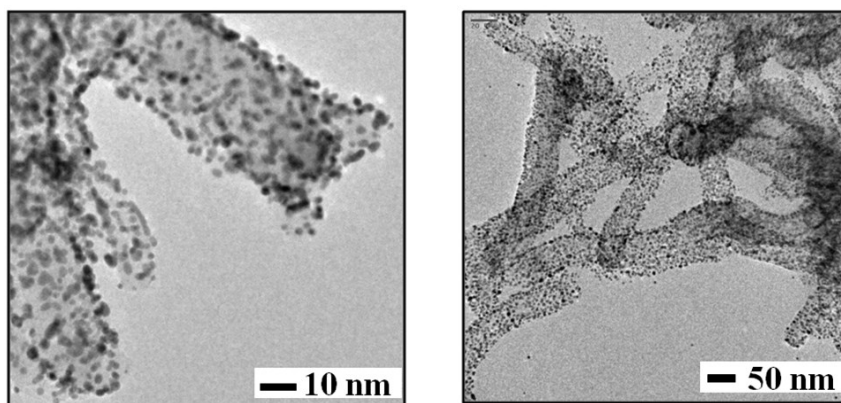
where R_1 and R_2 are particle radii; A is Hamaker constant.



(a)



(b)



(c)

Fig. S1. TEM micrographs: (a) NDT-linked Au NPs (6.1 ± 0.6 nm) assembly on C film. (b-c) TEM micrographs for NDT-Au_{nm} (6.0 ± 0.9 nm) on CNTs (d_{ee}), and the average interparticle edge-to-edge distance (d_{ee}) measured from image (b, left) $\sim 2.0 \pm 0.5$ nm.

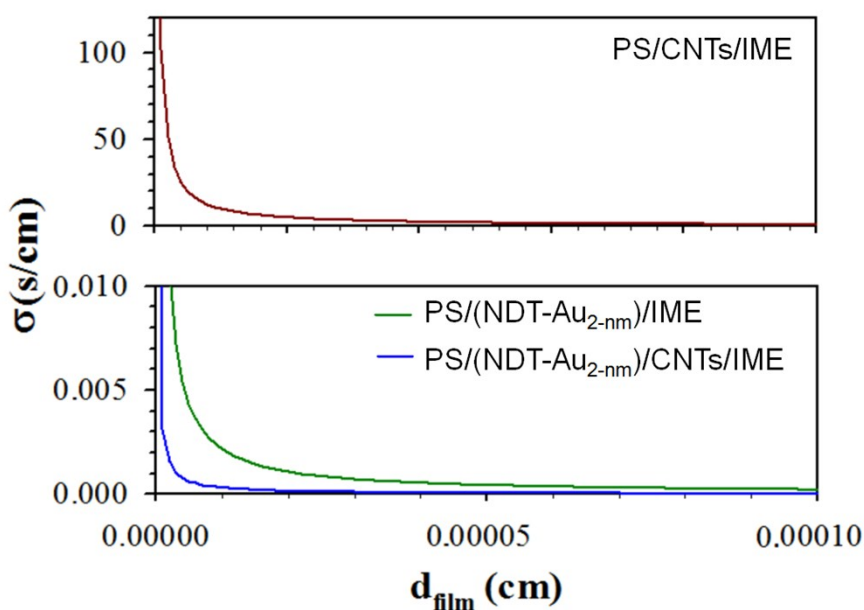


Fig. S2. Plots of the estimated electrical conductivity of the thin films on the IME device ($\sigma = (1/R)(w/dl)$) (R : resistance (Ω), d : film thickness (cm), l : microelectrode length (50 μm), and w : gap of the microelectrodes (5 μm)). Experimental resistances for thin films: $9.8 (\pm 1.1) \times 10^2 \Omega$ (PS/CNTs/IME), $4.6 (\pm 0.1) \times 10^6 \Omega$ (PS/(NDT-

$\text{Au}_{\text{nm}}/\text{IME}$), and $3.2 (\pm 0.1) \times 10^7 \Omega$ (PS/(NDT- Au_{nm})/CNTs/IME).

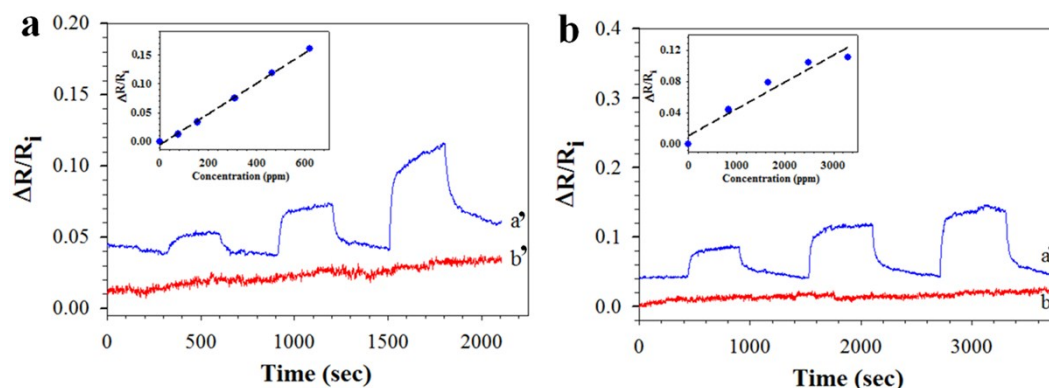


Fig. S3. (a) Response profiles of toluene (a) and hexane (b) vapors of increasing concentrations at: (NDT- $\text{Au}_{\text{nm}}/\text{CNTs}/\text{IME}$) (a') and at CNTs/IME (b'). Insert: a plot of the response vs. toluene concentration (ppm (M)) with linear regression slope: 2.6×10^{-4} (a) and 3.4×10^{-5} (b). (Estimated average 3x noise level: 0.0048).

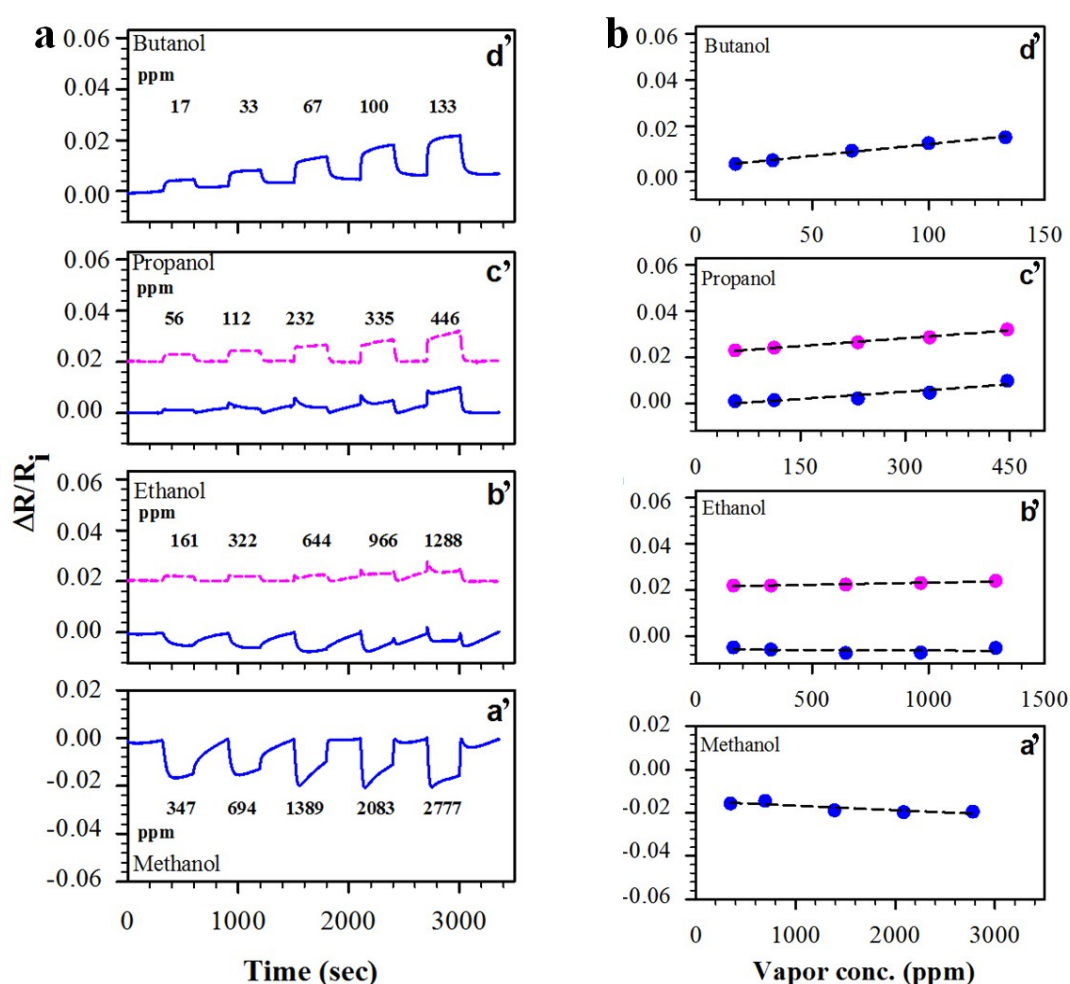


Fig. S4. (a) Response profiles of (NDT- $\text{Au}_{\text{nm}}/\text{IME}$) in response to different R-OH vapors (MeOH (a', vapor concentrations: 347, 694, 1389, 2083, 2777 (in ppm (M))), EtOH (b', vapor concentrations: 161, 322, 644, 966, 1288 (in ppm (M))), PrOH (c', vapor concentrations: 56, 112, 232, 335, 446 (in ppm (M))) and BuOH (d', vapor concentrations: 17, 33, 67, 100, 133 (in ppm (M))). (b) Plots of the response vs. concentration of different R-OH

vapors (ppm in moles per liter) at (NDT-Au_{nm})/CNTs/IME (linear regression slopes: -2.1×10^{-6} (a'); -4.6×10^{-7} and 1.8×10^{-6} (b'); 2.1×10^{-5} and 2.3×10^{-5} (c'), and 1.0×10^{-4} (d')). (Estimated average 3x noise level: 0.0006).

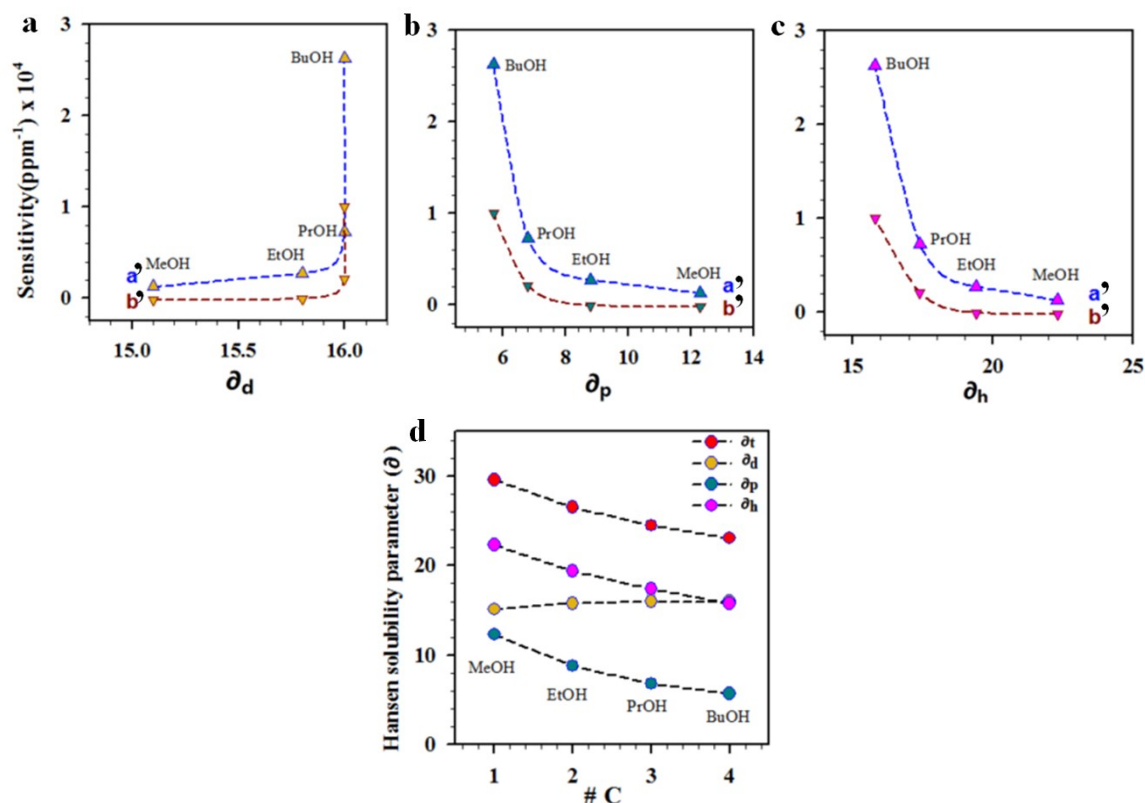


Fig. S5. (a-c) Plots of response sensitivities for a series of alcohol (R-OH) with (NDT-Au_{nm})/CNTs/IME (a', blue) and (NDT-Au_{nm})/IME (b', red) vs. the individual components in the solubility parameter ($\partial_t = \sqrt{\partial_d^2 + \partial_p^2 + \partial_h^2}$) for the VOCs. (d) Solubility parameters vs. #C in the alcohol molecules.

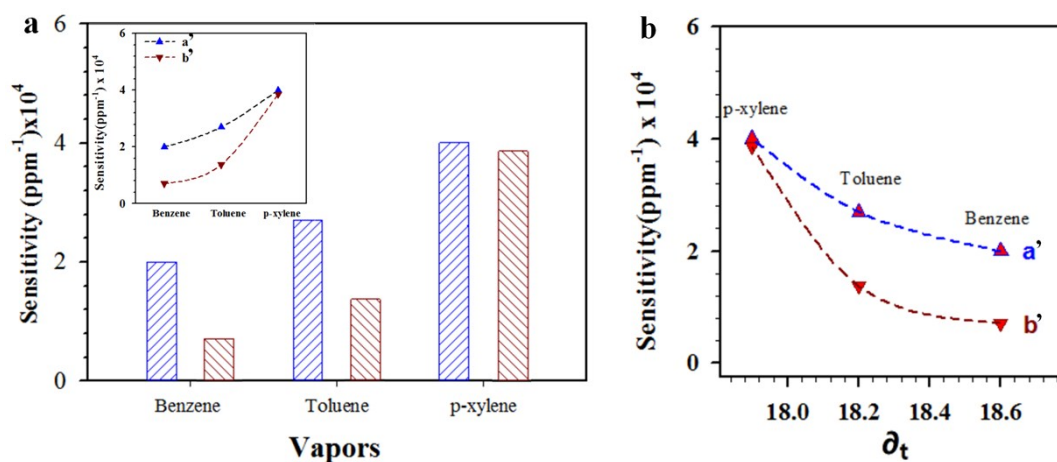


Fig. S6. (a) Comparison of response sensitivities for benzene, toluene, and p-xylene with (NDT-Au_{nm})/CNTs/IME (blue bars) and (NDT-Au_{nm})/IME (red bars). Inset: plots of the response sensitivity for the different vapor molecules ((a') (NDT-Au_{nm})/CNTs/IME); and (b') (NDT-Au_{nm})/IME). (b) Plots of the response sensitivity vs. total solubility parameter ((a') (NDT-Au_{nm})/CNTs/IME); and (b') (NDT-Au_{nm})/IME).

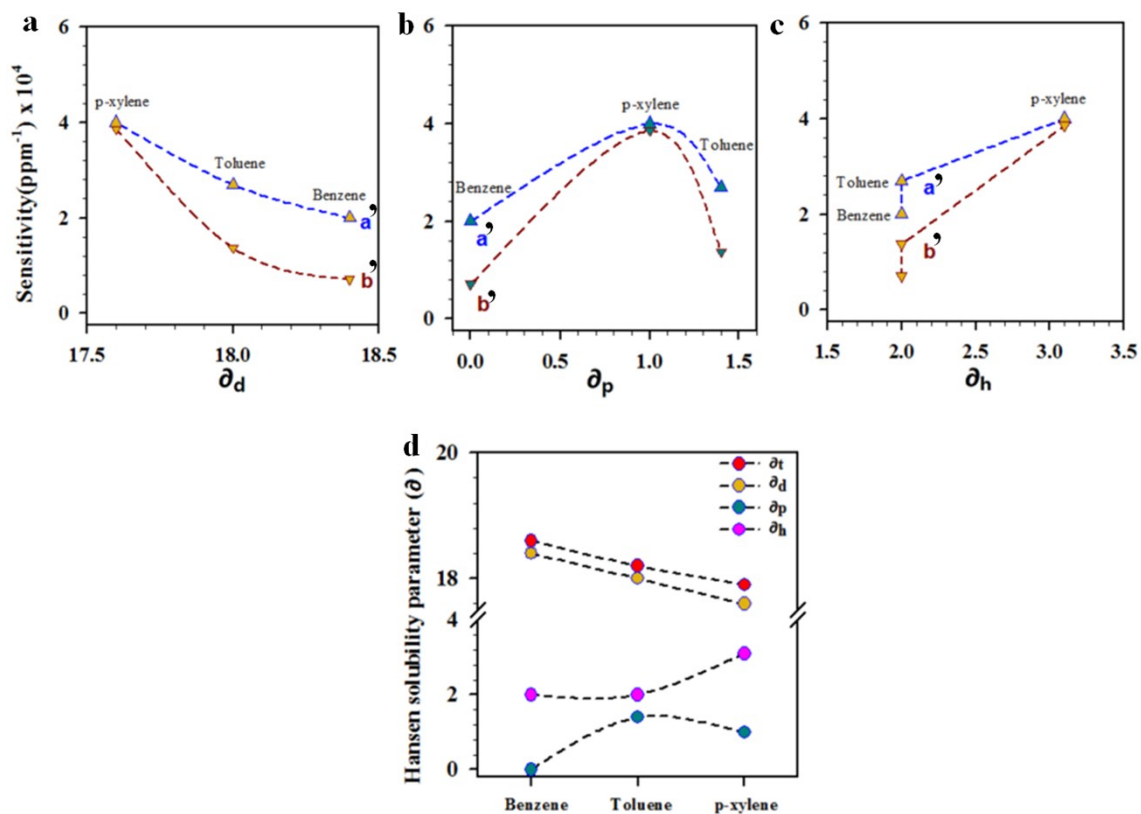


Fig. S7. (a-c) Plots of the response sensitivities for benzene, toluene and p-xylene vapors with (NDT-Au_{nm})/CNTs/IME (a', blue) and (NDT-Au_{nm})/IME (b', red) vs. the individual components in the solubility parameter ($\partial_t = \sqrt{\partial_d^2 + \partial_p^2 + \partial_h^2}$) for the VOCs. (d) Solubility parameters for the three different VOC molecules.